Superconductor Science and Technology

PAPER

Progress in scale-up of *RE*BCO STAR™ wire for canted cosine theta coils and future strategies with enhanced flexibility

To cite this article: Soumen Kar *et al* 2020 *Supercond. Sci. Technol.* **33** 094001

IOP Publishing Superconductor Science and Technology
Supercond. Sci. Technol. **33** (2020) 094001 (12pp) https://doi.org/10.1088/1361-6668/ab9e41

Progress in scale-up of *RE*BCO STAR™ wire for canted cosine theta coils and future strategies with enhanced flexibility

Soumen Kar[1,2], Jithin Sai Sandra[1], Wenbo Luo[2], Vamsi Yerraguravagari[2], Eduard Galstyan[2], Jan Jaroszynski[3], Dmytro Abraimov[3], Goran Majkic[2] and Venkat Selvamanickam[2]

[1] AMPeers LLC, Technology Bridge, University of Houston, Houston, TX 77023, United States of America
[2] Department of Mechanical Engineering, Advanced Manufacturing Institute, Texas Center for Superconductivity, University of Houston, Houston, TX 77204, United States of America
[3] Applied Superconductivity Center, National High Magnetic Field Laboratory, Florida State University, Tallahassee, FL 32310, United States of America

E-mail: skar2@uh.edu

Received 7 January 2020, revised 28 May 2020
Accepted for publication 18 June 2020
Published 15 July 2020

Abstract

We report recent developments in the scale-up of symmetric *RE*-Ba-Cu-O (*RE*BCO) tapes with 15–22 μm thick substrates. Using these symmetric *RE*BCO tapes, we fabricated up to 10 m long, symmetric tape round (STAR™) *RE*BCO wires, less than 2 mm diameter, using 1.02 mm and 0.81 mm diameter copper formers. The critical current of the long STAR™ wires made in lengths of 2–10 m ranges from 465 A to 564 A at 77 K, self-field. This wire was then used to construct a single-layer, full-depth groove, three-turn canted cosine theta (CCT) coil with a minimum bend radius of 15 mm. This three-turn CCT coil retains 95% of its I_c even when wound at a such a small bend radius. This result confirms the capability of fabricating CCT coils with STAR™ wire at a tilt angle of 30º which would yield a dipole transfer function of 0.48 T kA^{-1} at a 15 mm bend radius. Further, the architecture of STAR™ wire was modified for an I_c retention of >90% at an even smaller bend radius of 10 mm with the aim of increasing the dipole transfer function. The higher dipole transfer function enabled by STAR™ wire is an important step toward the eventual goal of a 5 T maximum dipole field in a *RE*BCO-based CCT coil. At a bend radius of 10 mm, a six-layer STAR™ wire exhibits a critical current of 288 A at 77 K, self-field, i.e. 94% I_c retention and 617 A at 4.2 K in a 15 T background field, which equals a J_e of 412.7 A mm^{-2} at a Lorentz force of 9.3 kN m^{-1}. This level of flexibility and the high performance of STAR™ wire in high fields at 4.2 K and with a small bend radius underscores its potential use in compact and low-cost high-field magnet and related applications.

Keywords: 2nd generation superconductor, canted cosine theta coil, dipole transfer function, Lorentz force, *RE*BCO, symmetric tape, STAR™ wire

(Some figures may appear in colour only in the online journal)

1. Introduction

The Large Hadron Collider (LHC) is now transitioning from using Nb-Ti dipoles to Nb_3Sn dipoles and quadrupoles to achieve higher operating magnetic fields for the High Luminosity LHC Upgrade (HL-LHC) [1–4]. Even higher gains in beam energy and luminosity can be obtained by using high-temperature superconductor (HTS) dipoles, which are the only option for field strengths in the vicinity of 20 T [5–10]. The development of practical, high-current- density round isotropic wires from $REBa_2Cu_3O_7$ (*RE*BCO, *RE* = rare earth) tapes, for use as a single strand conductor or as a sub-element of a complex cable, may constitute a real breakthrough in magnet technology [11]. *RE*BCO tapes have already been deployed in user-oriented high-field magnets for very high-field (30 T range) solenoids for laboratory measurements and new frontier nuclear magnetic resonance beyond 1 GHz [12, 13]. Canted cosine theta (CCT) beam steering magnets using a smaller bend radius winding configuration are a leading candidate for the generation of multipole magnetic fields employing helical current paths, and have gained interest from the U.S. Magnet Development Program (MDP) [14]. CCTs, and other magnets for accelerators, require superconductor tapes/wires several kilometers in length without any significant weak sections. *RE*BCO coated conductors are a leading candidate for HTS dipoles. Coated conductors are fabricated by a reel-to-reel continuous process that is amenable to low-cost manufacturing and have demonstrated a J_e over 5 kA mm^{-2} at 4.2 K, 14 T [15]. The high yield strength (> 700 MPa) of *RE*BCO coated conductors is especially beneficial for withstanding the intense forces in high magnetic fields [16]. In the U.S.A, magnet technology development is shifting its focus from single tapes [17–20] to multi-tape isotropic cables under the framework of the U.S. Magnet Development Program (USMDP). The USMDP, supported by the Office of High Energy Physics at the U.S. Department of Energy, has a dedicated component for the development of HTS accelerator magnet technology with the initial goal of demonstrating a magnet with a 5 T dipole field and measuring its field quality [21]. In the future, to generate > 5 T of dipole field at a background field of 15 T, six-layer CCT coils with a tilt angle of 20° yielding a dipole transfer function of 0.78 are desired, and will require a conductor bend radius of 10 mm [14, 21]. From reference [14], it is observed that the reduction in tilt angle and bend radius of the CCT coil reduces the J_e requirements of the conductor at 20 T drastically. Furthermore, a robust STAR™ wire, bendable to a 10 mm bend radius without significant I_c degradation, can be used in novel coil fabrication methods such as low-cost direct winding for complex high field magnet structures [22–26].

A challenge with *RE*BCO coated conductors as compared to Nb-Ti, Nb_3Sn and Bi-2212 wires is associated with their flat rather than round geometry and wide (~ 12 mm) profile rather than multifilamentary architecture. This challenge has been overcome using symmetric *RE*BCO tapes wherein the *RE*BCO film is positioned at the neutral plane [27–33]. Due to the excellent bend tolerance of the *RE*BCO symmetric tapes, the flat *RE*BCO tape geometry can be converted to round wire by the helical winding of narrow tapes on a round former as small as 0.51–1.02 mm [27–30]. AMPeers and the University of Houston demonstrated symmetric tape round (STAR™) *RE*BCO wires as small as 1.3–1.9 mm in diameter, suitable for bending at a 15 mm radius with >90% I_c retention, with a record J_e of 586 A mm^{-2} at 20 T, 4.2 K [31]. In this manuscript, we report the scaling up of STAR™ wires to 10 m lengths with a 15 mm bend radius capability as well as the recent development of STAR™ wire with a minimum 10 mm bend radius capability. The critical current (I_c) of these highly flexible STAR™ wires has been tested at 4.2 K in magnetic fields up to 31.2 T when bent to a 10 mm radius.

2. Experiments and results

2.1. Characteristics of 50 m long symmetric REBCO tapes

In order to fabricate up to 10 m long STAR™ wires, we produced 12 mm wide symmetric *RE*BCO tapes using 15–22 μm thick Hastelloy substrate. The tapes consist of ~200 nm thick buffer layers based on MgO made by ion beam assisted deposition, ~1.7 μm (Gd,Y)BCO superconductor film made by metal organic chemical vapor deposition with silver layers ~2 μm thick on the *RE*BCO film side and ~0.5 μm thick on the substrate side. The copper stabilizer was electroplated primarily on the *RE*BCO film side so as to position the film at the neutral plane. The copper thickness was adjusted to (18–30 μm) based on the substrate thickness as described in reference [28].

Reel-to-reel scanning Hall probe microscopy (SHPM) (B_{Peak} ~ 1 T) was used to characterize the uniformity of the tapes, with a resolution of 1 mm in the *X* direction (tape length) and 50 μm in the *Y* direction (tape width). Since SHPM provides a two-dimensional image of current flow at a resolution of about 10 μm, any defects that result in dropout in the critical current of the ultra-thin *RE*BCO tape can be identified. By better procedures to process the ultra-thin tapes, we have successfully scaled up the fabrication of 18 μm thick substrate *RE*BCO tape to 50 m lengths with dropouts in I_c of less than 10% as shown in figure 1(a). The uniformity in I_c over the whole length is 2.2%.

Figure 1(b) shows the trapped magnetic field map of the 50 m long tape in the 17.5–20.5 m section. The disruption of the trapped field on the upper side of the tape reveals a drop in I_c at 18.03–18.30 m and 18.93–19.75 m. Figure 1(c) shows the current density map as extracted from the magnetic field map and it shows the same trend as the field map.

In order to utilize smaller copper formers, the 12 mm wide ultra-thin substrate *RE*BCO tapes were laser slit to 1.4–2.6 mm widths. Hereafter, silver layers of 2–3 μm thickness on the *RE*BCO side and 1 μm on the substrate side were deposited by reel-to-reel magnetron sputtering to facilitate the electrodeposition of copper stabilizer. Appropriate shielding was employed in the reel-to-reel copper electroplating tool to minimize the dog-boning electroplating effect on the tapes [34]. An optimal shield was used to deposit copper stabilizer primarily on the *RE*BCO film side to fabricate the symmetric tapes. In these copper-plated symmetric tapes, *RE*BCO film is

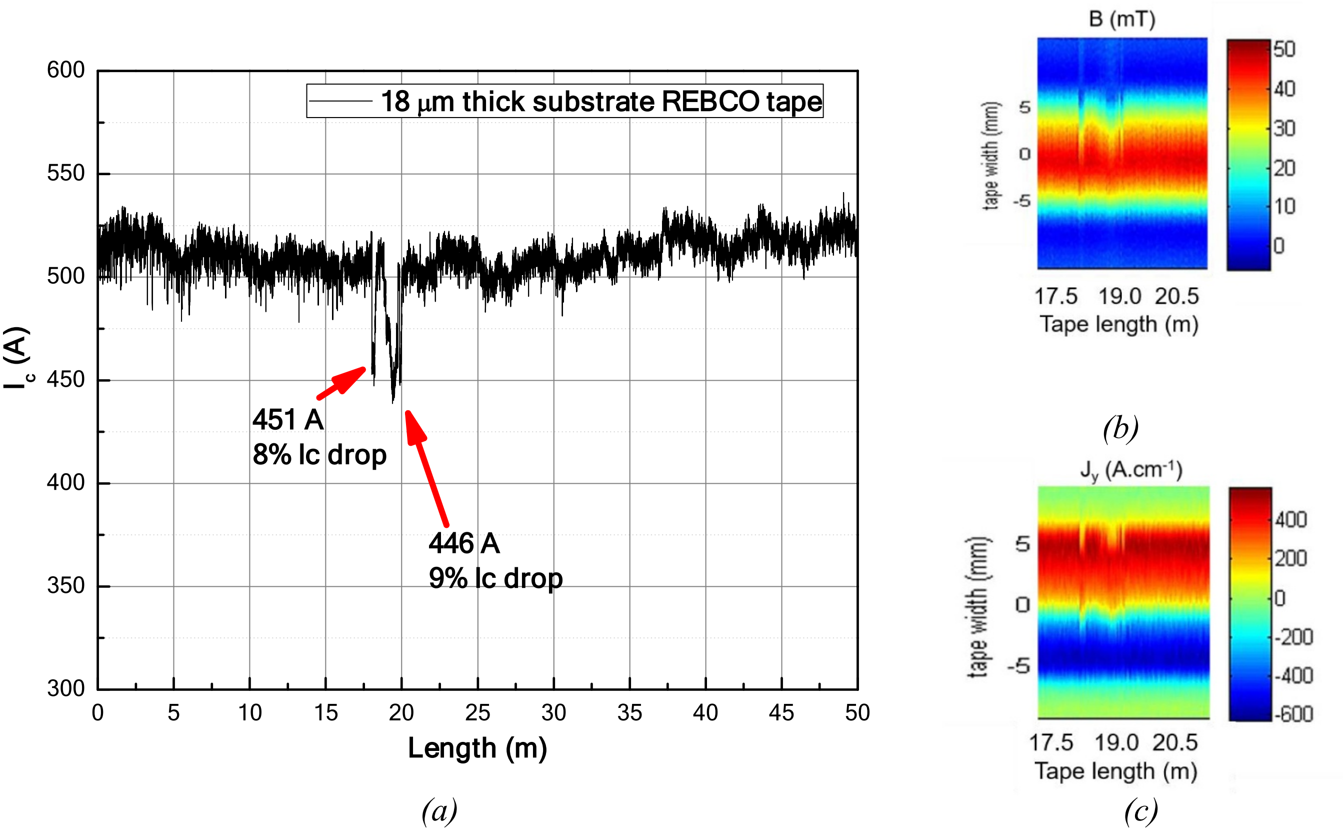

Figure 1. (a) I_c (77 K) over 50 m long, 12 mm wide, 18 μm substrate REBCO tape before copper plating, showing an I_c of 500 A with only two dropouts in I_c less than 10%; (b) trapped magnetic field map of the tape section at 17.5–20.5 m. (c) Current density map extracted from magnetic field map.

positioned near the neutral plane and experiences negligible strain while bending to a small bend radius [28–33]. As per our earlier reported elastoplastic model, the thickness of the electroplated copper stabilizer is individually adjusted for each tape layer in order to minimize bending strain as a function of layer radius [30].

Copper-electroplated symmetric *RE*BCO tapes 2.5 mm wide made with 18 μm thick substrate have been tested by SHPM in lengths up to 43 m. The 43 m long symmetric *RE*BCO tape exhibited an average critical current of 95 A at 77 K, self-field, with a uniformity of 4.9% as shown in figure 2. A trapped field map from a 1 m long section at the 14.5–15.5 m position is shown in figure 3, revealing uniform quality and the absence of defects that are usually readily discernible with SHPM.

2.2. Fabrication of STAR™ wires

Oxygen-free high-conductivity (OFHC) copper wires with diameters of 1.02 mm (18 AWG) and 0.81 mm (20 AWG) were selected as formers for the 2 m and 10 m long STAR™ wires, respectively, and 0.81 mm and 0.64 mm diameter (22 AWG) copper wires were selected as formers for the 25 cm long STAR™ wires. We had previously shown that this former is strong enough to withstand huge Lorentz forces (36 kN m^{-1}) in operation while flexible enough to bend the STAR™ wire to a small diameter [31–33]. The former had no insulation layer

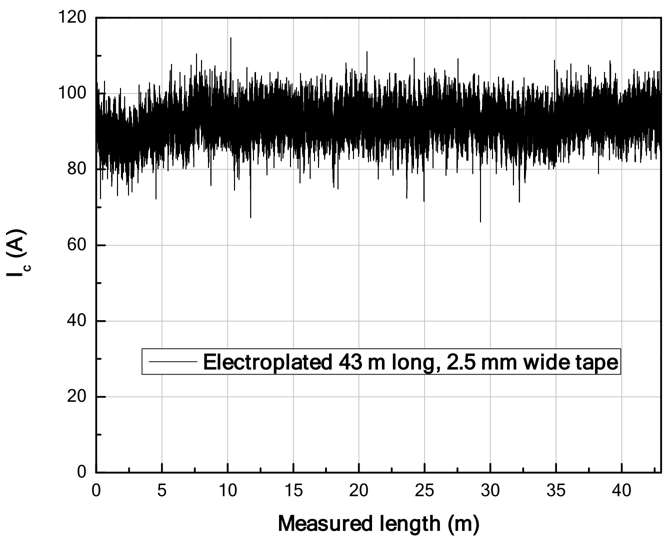

Figure 2. The SHPM measurement of I_c on a 43 m long, 2.5 mm wide, copper-electroplated symmetric tape at 77 K, self-field. The total thickness of tape is 50 μm, and the average I_c is 95 A.

to provide current-sharing ability. First, a 2.02 m long STAR™ wire was fabricated using eight layers of 2.4–2.6 mm wide, 45–60 μm thick symmetric *RE*BCO tape wound on 1.02 mm diameter copper wire former. Then, we fabricated five samples

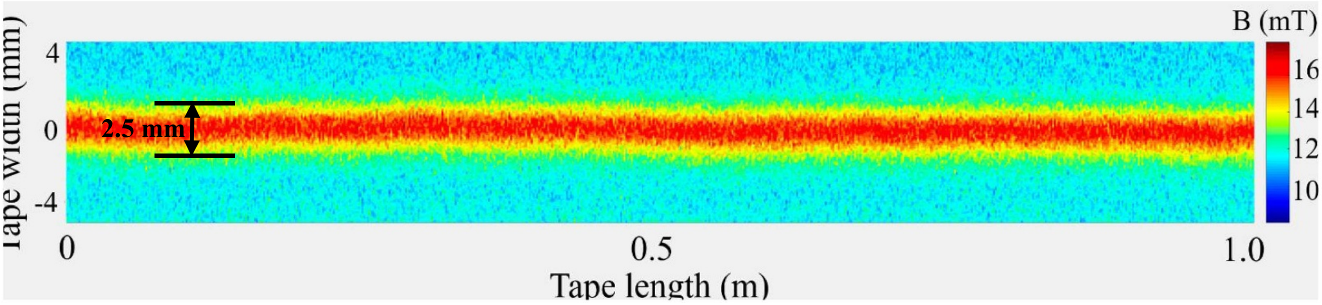

Figure 3. The SHPM magnetic field map of a 1.0 m long section at the 14.5–15.5 m position of a 43 m long, 2.5 mm wide, 18 μm thick substrate *RE*BCO symmetric tape.

of 2.0 m long STAR™ wire using a 0.81 mm diameter copper former to evaluate the feasibility of using a smaller diameter former for a higher *RE*BCO-to-copper ratio. The width and thickness of the symmetric tapes were varied in each layer in order to further optimize the mechanical properties, as described in table 1, for all long and short length STAR™ wire configurations.

Finally, a 10 m long STAR™ wire was fabricated by winding seven layers of 2.4–2.6 mm wide tapes on the 1.02 mm diameter Cu former, with narrower symmetric tapes and thinner substrate in the inner layers, and 2.6 mm wide symmetric tapes with 22 μm thick substrates in the outer layers. As explained in our previous publication, this new key feature of varied tape distribution has enabled significant improvements in the electric and mechanical performance of our STAR™ wires [31]. The terminals of the wires were made using indium-solder-filled copper ends. The final STAR™ wire diameter was measured using a micrometer (resolution: 0.001 mm and accuracy: 0.004 mm) every 0.5 m for the STAR™ (# 1 to # 6) and every 1 m for STAR™ wire # 7. The final diameter of the STAR™ wire was also verified using an optical microscope. It was observed using a micrometer that the final STAR™ wire diameter measurement was within ± 2% of the mean value.

To evaluate STAR™ wire bending performance at a 10 mm radius, we fabricated two wires using a 0.81 mm copper former and two wires of 0.64 mm. The width and thickness of the symmetric tapes were varied in each layer in order to achieve superior mechanical properties. Tapes with thinner substrates and narrower widths were wound in the inner layers of the wire, while the 18 μm thick substrate, 2.5 mm wide symmetric tapes (50 μm total thickness) were wound in the outer layers of STAR™ # 8 and # 9. The specifications of the fabricated 25 cm long STAR™ wires are listed in table 2. In particular, STAR™ wire # 10 was wound with two tapes of 1.4 mm width and then four tapes of 1.7 mm width, whereas STAR™ wire # 11 was wound with six tapes all of 1.7 mm width, in order to evaluate the feasibility of employing more gaps in the outer layers. All STAR wires (both long and short) were made with one tape in each layer and the tape thickness was increased from the inner to the outer layers. All wires were fabricated using a custom-built winding machine built purposely for the winding of STAR™ wires with a high level of accuracy. The tapes were wound with the thicker copper stabilizer on the *RE*BCO side facing inward, with a wrap angle of 45°. The gap between turns was increased progressively with the tape layer number, in order to increase the cooling efficiency and transversal flexibility of the STAR wire, allowing them to be bent to a small radius of 10 mm. The downside is that increasing the gap size reduces tape support, making the outer layers more susceptible to deformation due to Lorentz force. This is different from previous STAR™ wires where a constant tape geometry was used in each layer [32, 33]. Figures 4(a) and (b) show a photograph of STAR™ #1 and #7, respectively.

(a)

(b)

Figure 4. (a) STAR™ # 1 wire with 1.93 mm diameter, (b) STAR™ # 7 wire with 1.90 mm diameter before shrink tubing and 2.80 mm diameter after shrink tubing.

Table 1. Specifications of long STAR™ wires.

STAR™ #	Length	Former diameter, (AWG)	Tape width in each layer	Tape thickness	Total no. of layers (tapes)	Total tape width	Final STAR™ wire diameter
1	2.02 m	1.02 mm (18)	2.4 mm × 2, 2.5 mm × 2, 2.6 mm × 4	Variable across layers (~ 45–60 μm)	8 (8)	20.2 mm	1.93 mm
2 3 4 5 6	2 m	0.81 mm (20)	1.8 mm × 2, 2.2 mm × 2, 2.5 mm × 2, 2.6 mm × 2			18.2 mm	1.78 mm 1.77 mm 1.74 mm 1.75 mm 1.73 mm
7	10.48 m	1.02 mm (18)	2.4 mm × 2, 2.5 mm × 2, 2.6 mm × 3		7 (7)	17.6 mm	1.90 mm (before shrink tubing) 2.80 mm (after shrink tubing)
8		0.81 mm (20)	1.8 mm × 2, 2.5 mm × 4			13.6 mm	1.68 mm
9			1.4 mm × 2, 1.8 mm × 2, 2.5 mm × 2			11.4 mm	1.32 mm
10	25 cm	0.64 mm (22)	1.4 mm × 2, 1.7 mm × 4	Variable across layers (~ 32–50 μm)	6 (6)	9.6 mm	1.36 mm
11			1.7 mm × 6			10.2 mm	1.38 mm

Table 2. Design parameters for the full-depth three-turn CCT coil former.

Inner diameter (mm)	50
Outer diameter (mm)	60
Former material	Acura® Bluestone®
Turns	3
Tilt angle (degree)	30
Former length (mm)	350
Former thickness (mm)	5
Minimum bending diameter at magnet pole (mm)	30
Groove diameter (mm)	2.2
Groove depth (mm)	6.75
Rib thickness at the mid-plane (mm)	0.5

2.3. Transport critical current test set-up for long STAR™ wires

The I_c of the STAR™ wires (# 1 to # 6) were first measured at 77 K, self-field, in the form of a 25 cm diameter coil as shown in figure 5. For each STAR™ wire, every turn was properly isolated using Styrofoam spacers with voltage taps 1.8 m apart.

To check the I_c uniformity over the length, voltage taps were placed at every 0.5 m for STAR™ wire # 2. The wire was then tested in the form of a coil as shown in figure 5. All the STAR™ wires were tested in a liquid nitrogen bath at self-field. For testing STAR™ wire # 7, a 3D printed PLA-plastic cylinder 25 cm long, and with a 15 cm outer diameter was used as a mandrel to make a 22-turn, clear-bore solenoid as shown in figure 6(a). The voltage taps were placed every 100 cm as shown in figure 6(b). After all voltage tap connections, kapton tape was wrapped at several locations of the cylinder to ensure that STAR™ wire # 7 did not move from the grooves in the cylinder. The 77 K, self-field I_c test was performed on STAR™ wire # 7 in a liquid nitrogen bath before applying shrink tubing. First, the I_c was measured with V1 and V13 taps connected to the nanovoltmeter to obtain the overall wire I_c. As V1 and V13 were placed at the current contacts, a slight resistive transition was observed due to contact reistance. The measurements were then repeated between all adjacent taps (V_i–$V_{(i+1)}$), $i = 2$–12, spaced 100 cm apart with a stop current of 500 A.

Finally, STAR™ wire # 1 was used to make a three-turn full depth groove canted cosine theta (CCT) coil using a 35 cm long 3D printed coil former provided by Lawrence Berkeley National Laboratory (LBNL) as shown in figure 7, with the coil former specifications given in table 2. For the first time, a full-depth groove was used in the CCT coil former where STAR™ wires are placed deep inside the grooves. The groove depth of 6.75 mm (from the mandrel surface to the bottom of the groove) is used to accommodate multiple STAR™ wires. This full depth groove also helps during winding under tension and simplifies the impregnation of epoxy so that it can easily penetrate the groove. After impregnation, as the wire stays deep inside the groove, this arrangement prevents wire movement during tests due to additional support against Lorentz forces from all three sides of the groove. This CCT coil was tested at 77 K, self-field.

Table 3. Critical currents of long STAR™ wires at 77 K, self-field.

STAR™ #	STAR™ wire I_c (A)	J_e (A mm^{-2})
1	564	199
2	465	187
3	468	190
4	530	223
5	481	200
6	478	203
7	466	164

2.4. Transport critical current test set-up of short STAR™ wires for 10 mm bend radius

The short length STAR™ wires (# 8 to # 11) were first measured in a straight form for I_c at 77 K, self-field. The wires were then bent to a 10 mm radius half circle using a G10 mount. The I_c values of the bent form were obtained at both 77 K self-field and 4.2 K in-field. Figure 8 shows the G-10 sample holder assembly with STAR wire # 10 installed for bend testing before solder filling, with a wire length of 9 cm between the two copper terminals and a voltage tap spacing of 7 cm. The whole STAR wire was solder-filled for in-field testing at 4.2 K as in our previous report [31].

All 4.2 K tests were performed in a 31.2 T, 50 mm bore magnet at NHMFL. The magnetic field was perpendicular to the middle part of the sample, which was positioned at the magnet center. The field distribution of the magnet ensured less than 3% variation of field strength along the bore axis in a range of ± 10 mm. The current polarity was selected such that Lorentz force applied on the wire was against the G10 mount.

2.5. Transport critical current of long STAR™ wires at 77 K, self-field

Figure 9 shows the *E–I* characteristics at 77 K, self-field of the STAR™ wires (# 1 to # 7). Their measured I_c values (1 μV cm^{-1}) are summarized in table 3.

For STAR™ wire # 2, we measured the I_c uniformity over the length from the voltage taps 0.5 m apart and the results are shown in figure 10. STAR™ wire # 2 shows an average I_c of 465 A and a minimum I_c of 436 A. The maximum I_c is 5.8% higher than the average I_c and the minimum I_c is 6.2% lower than the average I_c.

For STAR™ wire # 7, we measured the I_c uniformity over the length from the voltage taps V2–V12 (figure 6(b)) after setting a stop current of 500 A. Figure 11 shows the I_c distribution over the length of STAR™ # 7. A minimum I_c of 436 A (77 K, self-field) was measured. Several segments did not show resistive transition before the tests were halted. An end-to-end I_c of 466 A was measured between V1 and V13. So, the minimum I_c of STAR™ wire # 7 is 6.4% lower than the end-to-end I_c.

Figure 5. The 77 K self-field I_c test of STAR™ wire # 1 in the form of a 25 cm diameter coil.

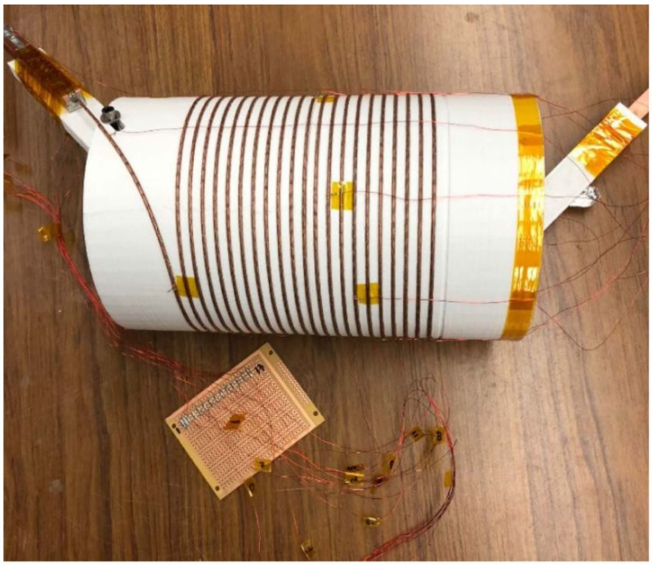

(a)

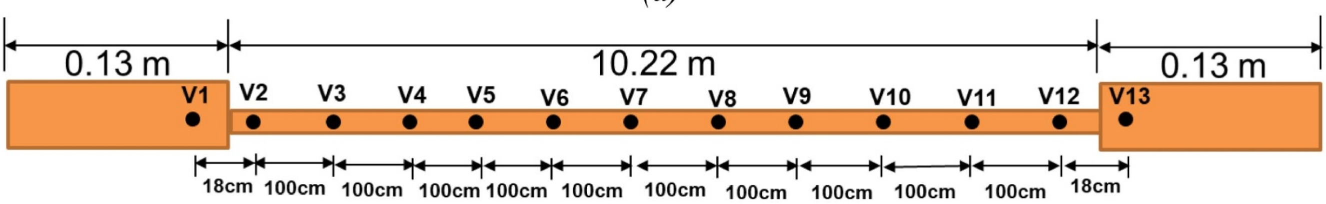

(b)

Figure 6. (a) STAR™ wire #7 wound over 22 turns on a 25 cm long, 15 cm diameter 3D-printed mandrel for critical current measurement; (b) multiple voltage tap locations of the STAR™ wire for checking I_c uniformity over the length at 77 K, self-field.

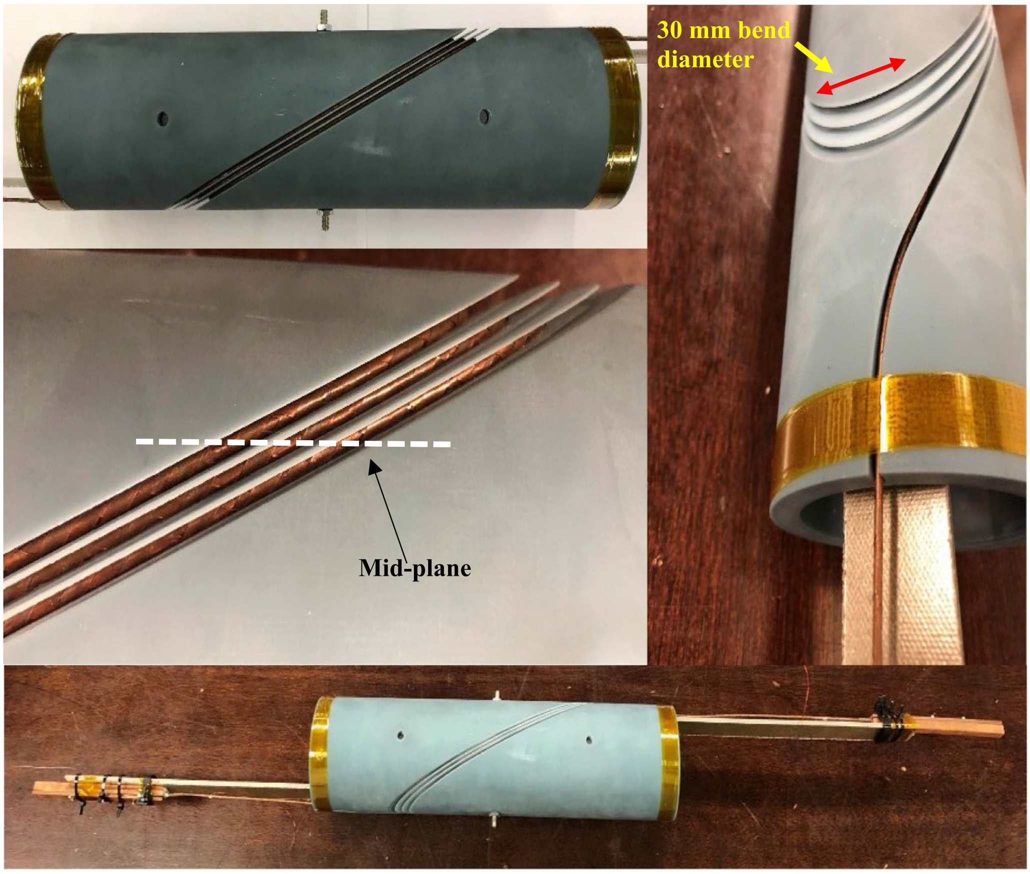

Figure 7. A three-turn, full-depth groove canted cosine theta (CCT) coil made with STAR™ wire using a 35 cm long 3D printed coil former provided by Lawrence Berkeley National Laboratory (LBNL) and its end connections. The white dashed line represents the mid-plane of the CCT coil.

Figure 8. G-10 sample holder 19 mm in diameter with STAR wire # 10 mounted for 20 mm bend test.

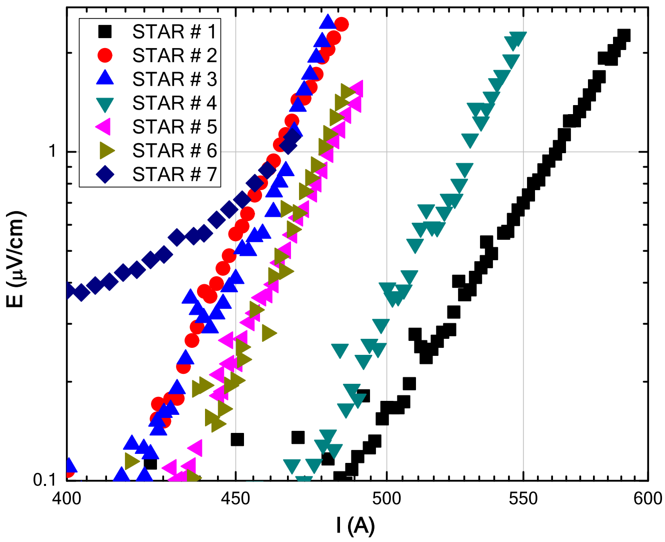

Figure 9. *E–I* plots at 77 K, self-field of STAR™ wires (#1 to #7).

2.6. Transport critical current test of a three-turn full depth groove CCT coil at 77 K, self-field

STAR™ wire # 1 exhibited an I_c of 564 A, i.e. 199 A mm^{-2} at 77 K, self-field, before winding to the three-turn CCT coil. Figure 12 shows the *E–I* plot of the CCT coil exhibiting a I_c of 534 A, i.e. 188.4 A mm^{-2} at 77 K, self-field, which indicates 94.7% I_c retention even at a smaller bend diameter of 30 mm. Such a high critical current retention at such a small bend radius demonstrates the mechanical robustness of STAR™ wires for CCT coil fabrication.

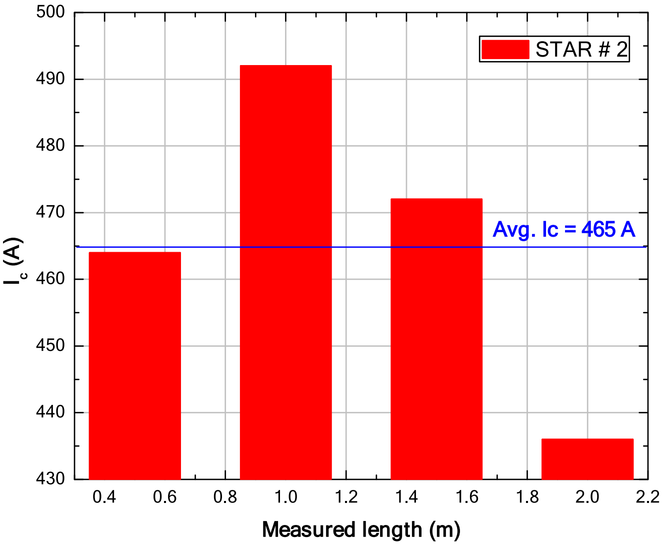

Figure 10. I_c distribution over the length of STAR™ # 2 with an average I_c of 465 A and min I_c of 436 A.

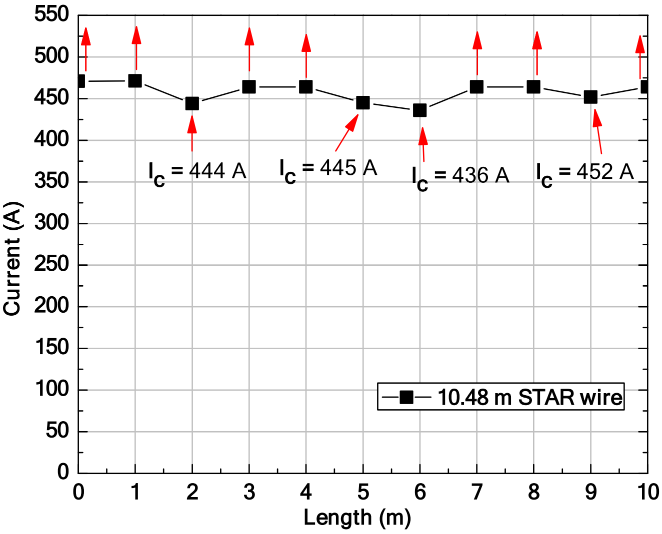

Figure 11. I_c distribution over the length of STAR™ # 7 with an overall I_c of 466 A and min I_c of 436 A at 77 K, self-field. The wire segments with data points and without I_c value labels did not show resistive transition at the current levels shown.

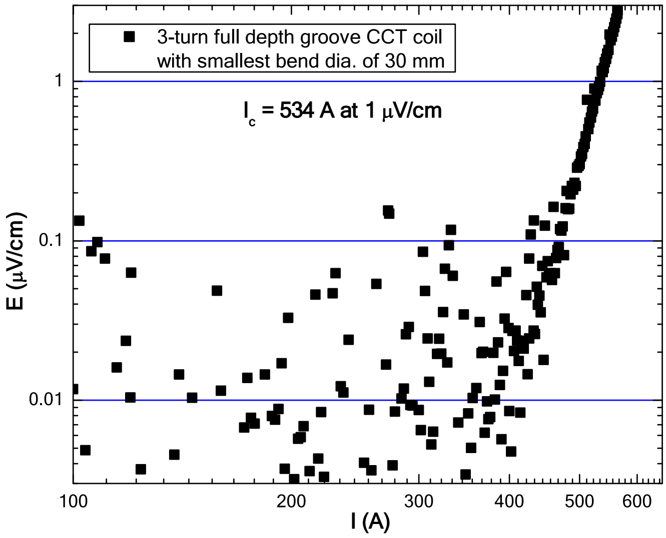

Figure 12. *E–I* plot of STAR™ wire #1 wound as a three-turn full depth groove CCT coil with the smallest bending diameter of 30 mm.

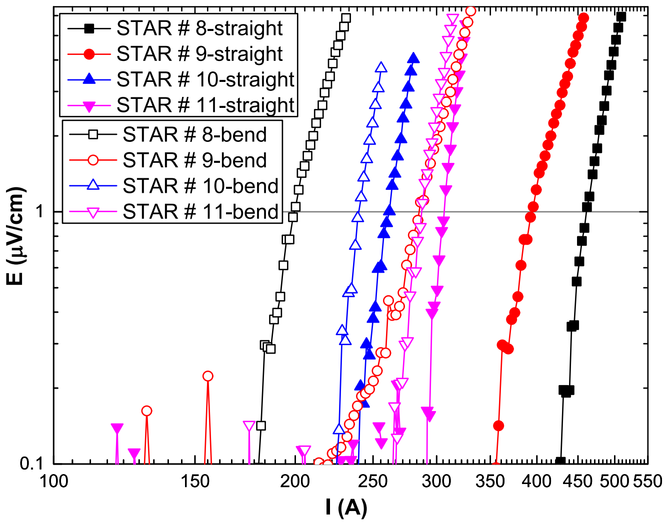

Figure 13. *E–I* characteristics of *RE*BCO STAR™ wires # 8 to # 11 at 77 K, self-field, in straight form (filled symbols), and 10 mm bending radius (open symbols).

2.7. Transport critical current at 77 K, self-field of short STAR™ wires at a bend radius of 10 mm

Figure 13 shows the *E–I* characteristics at 77 K, self-field of STAR™ wires # 8 to # 11 in a straight form and at a 10 mm bend radius, respectively. As the I_c of the symmetric tapes used for the fabrication of STAR™ wires was in the range of 30–38 A mm^{-1}, the results reveal 90%–95% I_c retention after winding the tapes on the STAR™ wires. The measured I_c values (1 μV cm^{-1}) of the *RE*BCO STAR™ wires in straight form and at 10 mm bend radius are summarized in table 4.

In straight form, STAR # 8 showed a I_c of 462 A and STAR # 9 showed an I_c of 396 A, whereas at 10 mm bending radius they exhibited a I_c of 200 A and 285 A, respectively, which corresponds to an I_c retention of 43.3% and 72% only. On the other hand, STAR # 10 and # 11 showed an I_c retention of 92% and 93.8% respectively. The low I_c retention of STAR # 8 and # 9 at a 10 mm bend radius must have been due to the use of a wider tape (2.5 mm) in the outer layers, which prevents the sliding of tapes between adjacent turns due the insufficient space. By using narrow tape (1.7 mm) in the outer layers in STAR # 10 or tapes of fixed width of 1.7 mm in STAR # 11, the tapes in the outer layers have enough space to slide without overlapping resulting in a significant increase in the I_c retention in these wires.

Table 4. The critical currents of STAR™ wires at 77 K, self-field, in straight form and at 10 mm bend radius.

STAR #	I_c (A) in straight form	J_e (A mm^{-2}) in straight form	I_c (A) at 10 mm bend radius	J_e (A mm^{-2}) at 10 mm bend radius	Retention of I_c at 10 mm bend radius
8	462	208.6	200	90.3	43.3%
9	396	289.7	285	208.5	72%
10	262	180.4	241	166	92%
11	307	205.4	288	192.6	93.8%

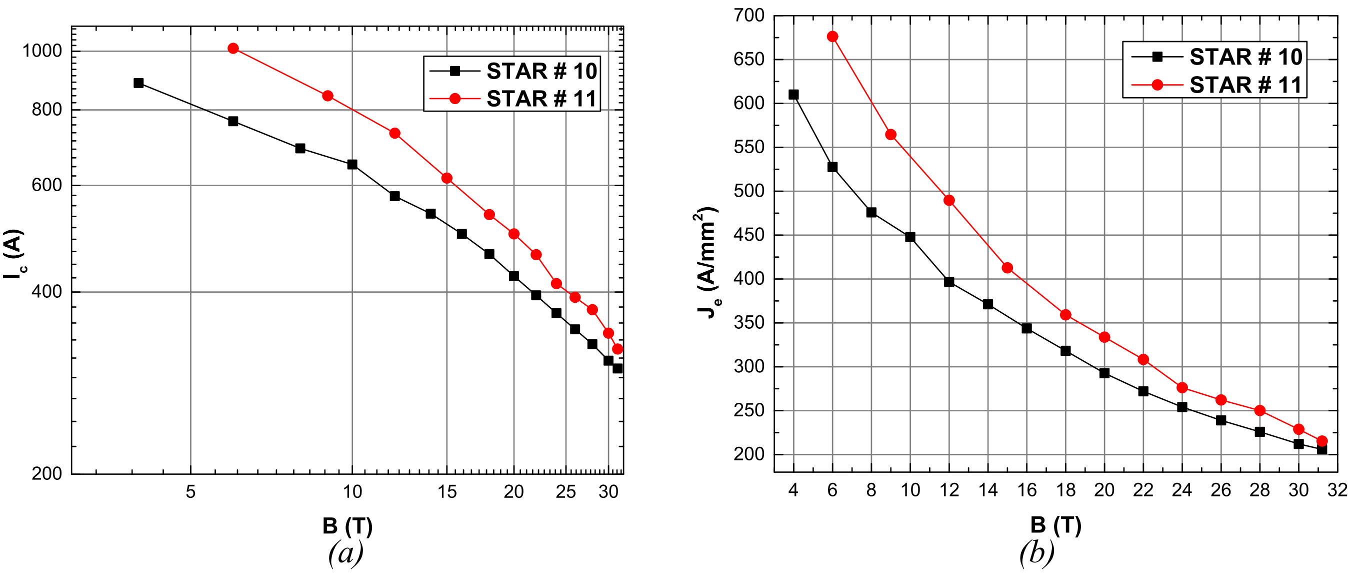

Figure 14. (a) The magnetic field dependence of I_c (at 1 μV cm^{-1}) for STAR wire # 10 and # 11; (b) J_e at different magnetic fields of STAR wire # 10 and # 11.

2.8. STAR™ wire performance at 4.2 K, in-field, at a bend radius of 10 mm

After 77 K measurements, the best STAR wires (# 10 and # 11) were tested in bent form (10 mm radius) at 4.2 K with an applied background magnetic field ranging from 4 T to 31.2 T to check performance under a huge Lorentz force. For >18 T measurements, after each measurement, the field ramped down to 18 T for helium stabilization, i.e. to suppress bubble formation. The maximum current limit of the DC power supplies was 1400 A. In certain low-field measurements, pulse current mode was used to avoid overheating of the sample. The STAR wires were in good condition after in-field measurements and subsequent verification tests done at 77 K showed no degradation.

As shown in figure 14(a), STAR wires # 10 and # 11 showed an I_c of 425 A and 499 A at 20 T, 4.2 K, which corresponds to a Lorentz force (F_L) of 8.5 kN m^{-1} and 9.9 kN m^{-1} respectively. These STAR™ wires show a lift factor (I_c at 4.2 K, 20 T, I_c at 77 K, self-field) of 1.76 (STAR # 10) and 1.73 at 4.2 K, 20 T. STAR # 11 shows a 15% higher I_c likely due to having 6% more *RE*BCO tape width content.

STAR wires # 10 and # 11 show a J_e of 206 A mm^{-2} and 215 A mm^{-2} at Lorentz force (F_L) of 9.3 kN m^{-1} and 10 kN m^{-1} respectively at 4.2 K, 31.2 T. Repeated tests in this field showed the same level of performance confirming reproducibility. STAR wire # 11 exhibited a J_e of 333.7 A mm^{-2} at 20 T and 412.7 A mm^{-2} at 15 T, which are the highest reported values so far for *RE*BCO round wires at a 10 mm bend radius. For CCT coils, as the minimum bend radius decreases, the requirement of the high J_e also decreases to obtain a higher dipole transfer function [14]. Therefore, the newly configured highly flexible STAR™ wire is suitable for more compact CCT coils and due to the 15%–20% lower consumption of *RE*BCO tape, they are less expensive as well.

Figure 15 shows the progress in STAR™ wires developed over 2 years as well as their respective J_e and *RE*BCO tape consumption along with the minimum bend radius. The continued improvement of J_e and the minimum bend radius portray the potential of *RE*BCO STAR™ wire for use in compact high-field magnet and related applications.

3. Conclusions

We have successfully fabricated 50 m long *RE*BCO tapes with a 15–22 μm thick substrate showing I_c of 500 A 12 mm^{-1} width with <10% drop out and a good I_c uniformity of 2.16% over the entire length. The symmetric tapes were slit to a narrow width of 2–2.5 mm and copper plated primarily on the

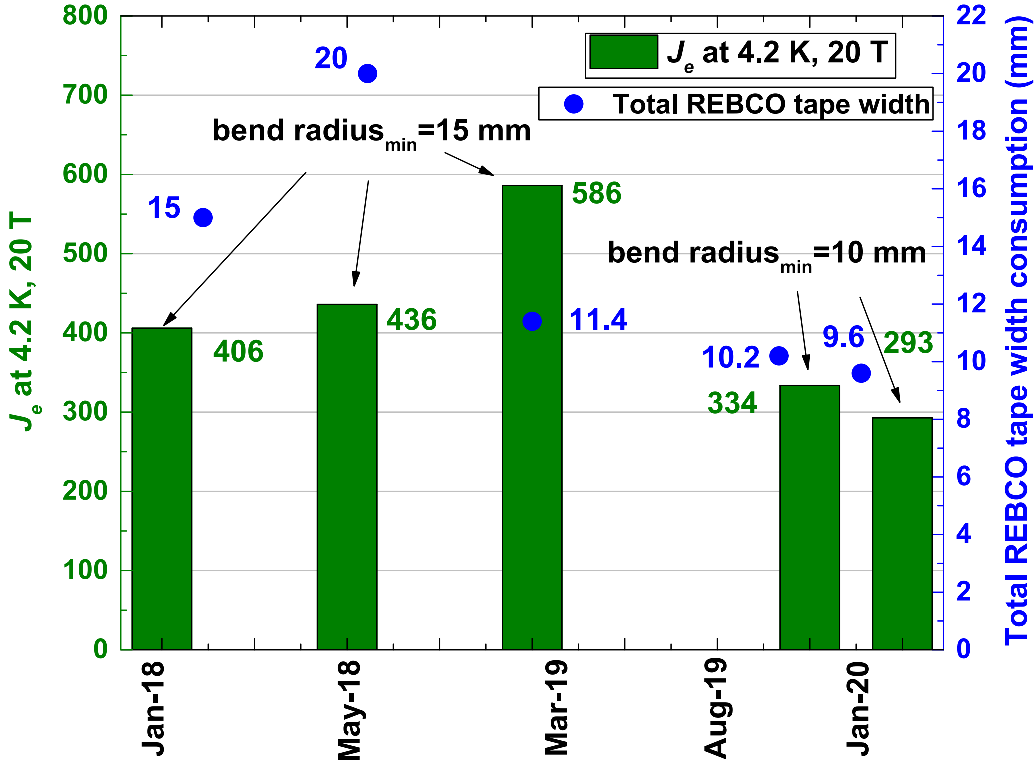

Figure 15. STAR™ wires developed over 2 years (from January 2018 to January 2020) and their respective J_e and *RE*BCO tape consumption (sum of all tape widths to make six- or eight-layer STAR wire) along with the minimum bend radius.

*RE*BCO film side to fabricate symmetric tapes. The symmetric tapes were used to fabricate six 2 m long STAR™ wire samples using 1.02 mm and 0.81 mm diameter copper former. These wires showed a I_c between 465 A and 564 A, which corresponds to a J_e of 187–223 A mm^{-2}. A 2.02 m long STAR™ wire (# 1) was then used to construct a single-layer, full-depth groove, three-turn CCT coil with a 15 mm minimum bend radius on a former provided by LBNL. This three-turn CCT coil with STAR™ wire exhibits a J_e of 188.4 A mm^{-2} and retains 94.7% of its I_c at 77 K, self-field, even when the wire is wound at a 15 mm bend radius. This result confirms the capability of fabricating CCT coils with a STAR™ wire at a tilt angle of 30°, which would yield a dipole transfer function of 0.48 T kA^{-1}. The higher dipole transfer function enabled by STAR™ wire is an important step toward the eventual goal of a 5 T maximum dipole field in a *RE*BCO-based CCT coil for the US MDP. A 10.48 m long STAR™ wire (#7) was fabricated with an end-to-end I_c of 466 A corresponding to a J_e of 164 A mm^{-2} at 77 K, self-field. Further, we developed a new type of STAR™ wire suitable for a 10 mm bend radius. J_e values of 333 A mm^{-2} and 412.7 A mm^{-2} were achieved with this wire at 20 T and 15 T, which are the highest levels reported in the data so far for *RE*BCO round wires at a 10 mm bend radius. The newly configured STAR™ shows an excellent J_e of 215 A mm^{-2} at a Lorentz force (F_L) of 10 kN m^{-1} at 4.2 K, 31.2 T without any degradation. These excellent results underscore the potential of *RE*BCO STAR™ wire for use in compact high-field magnets and related applications.

Acknowledgments

This work was supported by the US Department of Energy (DOE)—SBIR awards DE-SC0015983 and DE-SC0018850. A portion of this work was performed at the National High Magnetic Field Laboratory, which is supported by the National Science Foundation Cooperative Agreement No. DMR-1644779 and the State of Florida. We thank Muhammad Muneeb Siddique, Hugh Higley and Xiaorong Wang at LBNL for the three-turn CCT coil mandrel reported here.

One of the authors (VS) has financial interest in AMPeers LLC.

ORCID iDs

Soumen Kar https://orcid.org/0000-0001-5550-6859
Eduard Galstyan https://orcid.org/0000-0003-1486-6449
Jan Jaroszynski https://orcid.org/0000-0003-3814-8468
Goran Majkic https://orcid.org/0000-0003-0168-0856
Venkat Selvamanickam https://orcid.org/0000-0001-6618-9406

References

[1] Durante M *et al* 2018 Realization and first test results of the EuCARD 5.4-T *RE*BCO dipole magnet *IEEE Trans. Appl. Supercond.* **28** art no 4203805

[2] Rossi L *et al* 2015 The EuCARD-2 future magnets project: the European collaboration for accelerator quality HTS magnets *IEEE Trans. Appl. Supercond.* **25** art no 4001007

[3] Kirby G *et al* 2016 Status of the demonstrator magnets for the EuCARD-2 future magnets project *IEEE Trans. Appl. Supercond.* **26** art no 4003307

[4] Bottura L, de Rijk G, Rossi L and Todesco E 2012 Advanced accelerator magnets for upgrading the LHC *IEEE Trans. Appl. Supercond.* **22** art no 4002008

[5] Todesco E, Bottura L, de Rijk G and Rossi L 2014 Dipoles for high-energy LHC. presented at MT-23 *IEEE Trans. Appl. Supercond.* **24** also in CERN ATS 2014-0037 (2014)

[6] Rossi L 2011 LHC upgrade plans: options and strategy presented at the international conference on accelerators *Proc. of IPAC2011* (*San Sebastian, Spain*) pp 908–12 http://accelconf.web.cern.ch/AccelConf/IPAC2011/papers/tuya02.pdf

[7] Rossi L 2014 *First Workshop on Accelerator Magnets in HTS (WAMHTS-1)* (May21-23) (CERN: Hamburg, Germany) http://indico.cern.ch/event/308828/session/10/contribution/39

[8] Rossi L *et al* 2018 The EuCARD2 future magnets program for particle accelerator high-field dipoles: review of results and next steps *IEEE Trans. Appl. Supercond.* **28** art no 4001810

[9] Tommasini D *et al* 2017 The 16 T dipole development program for FCC *IEEE Trans. Appl. Supercond.* **27** art no 4000405

[10] Xu Q *et al* 2016 20-T dipole magnet with common-coil configuration: main characteristics and challenges *IEEE Trans. Appl. Supercond.* **26** 4000404

[11] Rossi L 2019 Small REBCO isotropic round wire (STAR): an important step from performant material to practical conductor in high field HTS magnets *Supercond. Sci. Technol.* **32** art no 100501

[12] Weijers H W *et al* 2016 Progress in the development and construction of a 32-T superconducting magnet *IEEE Trans. Appl. Supercond.* **26** art no 4300807

[13] Iwasa Y, Bascunan J, Hahn S, Voccio J, Kim Y, Lecrevisse T, Song J and Kajikawa K 2015 A high-resolution 1.3-GHz/54-mm LTS/HTS NMR magnet *IEEE Trans. Appl. Supercond.* **25** art no 4301205

[14] Wang X *et al* 2018 A viable dipole magnet concept with REBCO CORC® wires and further development needs for high-field magnet applications *Supercond. Sci. Technol.* **31** art no 045007

[15] Majkic G, Pratap R, Xu A, Galstyan E, Higley H C, Prestemon S O, Wang X, Abraimov D, Jaroszynski J and Selvamanickam V 2018 Engineering current density over 5 kA mm^{-2} at 4.2 K, 14 T in thick film REBCO tapes *Supercond. Sci. Technol.* **31** art no 10LT01

[16] Selvamanickam V, Xie -Y-Y and Reeves J 2007 Progress in scale-up of 2G wire at super power *Superconductivity for Electric Systems 2007 DOE Annual Peer Review* www.superpower-inc.com/files/pdf/2007PeerRev2G.pdf

[17] Amemiya N *et al* 2018 Coupling time constants of striated and copper-plated coated conductors and the potential of striation to reduce shielding-current-induced fields in pancake coils *Supercond. Sci. Technol.* **31** art no 10LT01

[18] Gupta R *et al* 2002 R&D for accelerator magnets with react and wind high temperature superconductors *IEEE Trans. Appl. Supercond.* **12** 75–80

[19] Gupta R *et al* 2015 Hybrid high-field cosine-theta accelerator magnet R&D with second-generation HTS *IEEE Trans. Appl. Supercond.* **25** art no 4003704

[20] Gupta R *et al* 2015 HTS quadrupole for FRIB–design, construction and test results *IEEE Trans. Appl. Supercond.* **25** art no 4603306

[21] Wang X, Gourlay S A and Prestemon S O 2019 Dipole magnets above 20 tesla: research needs for a path via high-temperature superconducting *RE*BCO conductors *Instruments* **3** 62

[22] Parker B, Anerella M, Escallier J, Ghosh A, Jain A, Marone A, Muratore J and Wanderer P 2012 BNL direct wind superconducting magnets *IEEE Trans. Appl. Supercond.* **22** art no 4101604

[23] Wanderer P and Parker B 2006 Direct wind slim quadrupoles for an LHC upgrade *LHC-LUMI-06 Proc.* pp 210–1 (https://cds.cern.ch/record/1045227/files/p210.pdf)

[24] Parker B and Escallier J 2005 Serpentine coil topology for BNL direct wind superconducting magnets *IEEE Proc. of the 2005 Particle Accelerator Conf.* pp 737

[25] Parker B 2011 BNL direct wind magnets (www.bnl.gov/magnets/staff/Parker/docs/4FO-6/4FO-6-Parker-BNL-Direct-Wind-Magnets.pdf)

[26] Parker B *et al* 2010 a superconducting magnet upgrade of the ATF2 final focus Proc. of IPAC'10 (*Kyoto, Japan*) pp 3440–2(http://accelconf.web.cern.ch/AccelConf/IPAC10/papers/WEPE041.pdf)

[27] Kar S, Luo W and Selvamanickam V 2017 Ultra-small diameter round REBCO wire with robust mechanical properties *IEEE Trans. Appl. Supercond.* **27** art no 6603204

[28] Kar S, Luo W, Sandra J S, Majkic G and Selvamanickam V 2019 Optimum copper stabilizer thickness for symmetric tape round (STAR) *RE*BCO wires with superior mechanical properties for accelerator magnet applications *IEEE Trans. Appl. Supercond.* **29** art no 6602605

[29] Luo W *et al* 2017 Fabrication and electromagnetic characterization of ultra-small diameter REBCO wires *IEEE Trans. Appl. Supercond.* **27** art no 6602705

[30] Yahia A B *et al* 2019 Modeling-driven optimization of mechanically robust *RE*BCO tapes and wires *IEEE Trans. Appl. Supercond.* **29** 8401605

[31] Kar S, Sandra J S, Luo W, Kochat M, Jaroszynski J, Abraimov D, Majkic G and Selvamanickam V 2019 Next-generation highly flexible round REBCO STAR wires with over 580A mm^{-2} at 4.2 K, 20 T for future compact magnets *Supercond. Sci. Technol.* **32** art no 10LT01

[32] Kar S, Luo W, Ben Yahia A, Li X, Majkic G and Selvamanickam V 2018 Symmetric tape round REBCO wire with J_e (4.2K, 15T) beyond 450 A/mm^2 at 15 mm bend radius: a viable candidate for future compact accelerator magnet applications *Supercond. Sci. Technol.* **31** art no 059601

[33] Luo W, Kar S, Li X, Galstyan E, Kochat M, Sandra J S, Jaroszynski J, Abraimov D and Selvamanickam V 2018 Superior critical current of symmetric tape round (STAR™) REBCO wires in ultra-high back-ground fields up to 31.2T *Supercond. Sci. Technol.* **31** art no 12LT01

[34] Floegel-Delor U, Riedel T, Rothfeld R, Schirrmeister P, Koenig R and Werfel F N 2016 High-efficient copper shunt deposition technology on REBCO tape surfaces *IEEE Trans. Appl. Supercond.* **26** art no 6603005